

# Chapter 5

## The Witten-Veneziano formula

In this chapter we show an alternative way to obtain  $F_\pi$  and we compare the result with the value obtained in the last chapter. The method relies on the Witten-Veneziano formula [1, 2], which in 3-flavor QCD relates the mass of the  $\eta'$  meson with  $m_\eta$ ,  $m_\pi$ ,  $F_\pi$  and the *topological susceptibility*  $\chi_T$ , defined below. This formula comes from the leading order term of a  $1/N_c$  expansion, for large  $N_c$  (number of colors). The quark composition of  $\eta$  and  $\eta'$  is approximately

$$\eta \approx \frac{1}{\sqrt{6}} (\bar{u}u + \bar{d}d - 2\bar{s}s), \quad \eta' \approx \frac{1}{\sqrt{3}} (\bar{u}u + \bar{d}d + \bar{s}s). \quad (5.1)$$

In nature the  $\eta$  and  $\eta'$  states are mixed, so the actual composition is given in terms of a *mixing angle*  $\theta_P$

$$\begin{pmatrix} \eta \\ \eta' \end{pmatrix} = \begin{pmatrix} \cos \theta_P & -\sin \theta_P \\ \sin \theta_P & \cos \theta_P \end{pmatrix} \begin{pmatrix} \eta_8 \\ \eta_1 \end{pmatrix}, \quad (5.2)$$

where

$$\eta_8 = \frac{1}{\sqrt{6}} (\bar{u}u + \bar{d}d - 2\bar{s}s), \quad \eta_1 = \frac{1}{\sqrt{3}} (\bar{u}u + \bar{d}d + \bar{s}s). \quad (5.3)$$

$\eta_8$  belongs to an octet of states, while  $\eta_1$  to a singlet. The current measured value of  $\theta_P$  is  $-11.3^\circ$  [3].

The general version of the Witten-Veneziano formula in QCD reads

$$m_{\eta'}^2 - \frac{1}{2}m_\eta^2 - \frac{1}{2}m_\pi^2 = \frac{2N}{F_{\eta'}^2} \chi_T^{\text{que}}. \quad (5.4)$$

where  $N$  is the number of flavors,  $F_{\eta'}$  is the decay constant of the meson  $\eta'$  and “que” stands for quenched, *i.e.* its value when the fermion mass  $m \rightarrow \infty$ . According to ref. [1], to lowest order in a  $1/N_c$  expansion, we have  $F_{\eta'} = F_\pi$ . In the limit of massless fermions, eq. (5.4) is simplified for the Schwinger model<sup>1</sup> [4]

$$m_\eta^2 = \frac{2N}{F_\pi^2} \chi_T^{\text{que}}, \quad (5.5)$$

$\chi_T$  is defined for the Euclidean Schwinger model in the continuum as

$$\chi_T = \int d^2x \langle q(x)q(0) \rangle, \quad (5.6)$$

<sup>1</sup>The most suitable eta meson for two flavors would be  $\eta'$ , however, we will denote the meson as  $\eta$ .

where

$$q(x) = \frac{g}{4\pi} \epsilon_{\mu\nu} F_{\mu\nu}(x) = \frac{g}{2\pi} F_{12}(x) \quad (5.7)$$

is the *topological charge density*. With  $q(x)$  we define the *topological charge* as

$$Q = \int d^2x q(x). \quad (5.8)$$

We can formulate  $\chi_T$  in terms of  $Q$  as well

$$\chi_T = \frac{\langle Q^2 \rangle - \langle Q \rangle^2}{V}, \quad (5.9)$$

where  $V$  is the space-time volume. An important property of the topological charge is that it is an integer number. We can see that if we rewrite  $q(x)$  as a total divergence

$$q(x) = \partial_\mu \Omega_\mu(x), \quad \Omega_\mu(x) = \frac{g}{2\pi} \epsilon_{\mu\nu} A_\nu(x). \quad (5.10)$$

If we consider field configurations of finite action,  $F_{\mu\nu}(x)$  has to vanish at infinity, so the gauge field must be gauge equivalent to 0 when  $|x| \rightarrow \infty$

$$0 = A'_\mu(x) = A_\mu(x) - \frac{1}{g} \partial_\mu \varphi(x). \quad (5.11)$$

Then

$$Q = \int d^2x \partial_\mu \left( \frac{g}{2\pi} \epsilon_{\mu\nu} \frac{1}{g} \partial_\nu \varphi(x) \right) = \frac{1}{2\pi} \int_{\partial \mathbb{R}^2} d\sigma_\mu \epsilon_{\mu\nu} \partial_\nu \varphi(x), \quad (5.12)$$

where we have used the Gauss theorem. Now, if we consider a circumference of length  $L$ , we can identify  $Q$  with the following integral

$$\lim_{L \rightarrow \infty} \int_0^L dx U^*(x) \partial_x U(x), \quad \text{where} \quad U(x) = e^{i\varphi(x)}, \quad U(L) = U(0). \quad (5.13)$$

The last expression is equal to

$$\frac{1}{2\pi} [\varphi(L) - \varphi(0)] = n \in \mathbb{Z}, \quad (5.14)$$

hence  $Q$  is an integer.

As we mentioned in Chapter 3, we can relate  $m_\eta$  with the gauge coupling as follows

$$m_\eta^2 = N \frac{g^2}{\pi}. \quad (5.15)$$

Thus, by determining  $\chi_T$  we can obtain a value for  $F_\pi$ . To measure the topological susceptibility using lattice simulations, we have to discretize the topological charge density. This can be done through the plaquettes defined in Chapter 2. From eq. (2.96), we know that for a small lattice spacing  $a$ , the plaquettes have the following expression

$$U_{\mu\nu}(\vec{n}) = e^{iga^2 F_{\mu\nu}(\vec{n})}. \quad (5.16)$$

Then

$$F_{\mu\nu}(\vec{n}) = -\frac{i}{ga^2} \ln U_{\mu\nu}(\vec{n}). \quad (5.17)$$

That way, we have

$$q(\vec{n}) = -\frac{i}{2\pi a^2} \ln U_{12}(\vec{n}) \quad (5.18)$$

Ref.	$\chi_T^{\text{que}} g^2$	$F_\pi$
[4]	0.0253	0.3989
[7]	0.0300(8)	0.4342(58)
[8]	0.023	0.3801

Table 5.1: Topological susceptibility in different references. The results from refs. [8, 7] were obtained by means of lattice simulations, while in ref. [4]  $\chi_T^{\text{que}}$  was computed with an analytical treatment.

and

$$Q = \sum_{\vec{n} \in L} a^2 q(\vec{n}), \quad (5.19)$$

where  $L = \{\vec{n} = (n_1, n_2) | n_\mu = 0, 1, \dots, N_\mu - 1; \mu = 1, 2\}$  is the set of lattice sites.

The lattice configurations generated through Monte Carlo algorithms are sorted in different sectors, where each one is characterized by a topological charge. Furthermore, there is evidence (see e.g. refs. [5, 6]) that the distribution of these configurations corresponds approximately to a Gaussian function. Due to parity symmetry, we also have that

$$\langle Q \rangle = 0. \quad (5.20)$$

Then, one can calculate  $\chi_T$  on the lattice using the following weighted average

$$\chi_T = \frac{\sum_i Q_i^2 N_i}{V \sum_i N_i}, \quad (5.21)$$

where  $i$  denotes a sector with  $N_i$  configurations labeled by a topological charge  $Q_i$ .

In the last chapter we showed results of  $Q$  obtained with simulations for several lattice sizes, using low statistics ( $10^3$  measurements separated by 10 sweeps). We attempted to compute the topological susceptibility using those results. Unfortunately, even though the topological charge is compatible with  $\langle Q \rangle \approx 0$ ,  $\chi_T$  as a function of the fermion mass  $m$  does not have a clear behavior (see figure 5.1 for instance). This does not allow us to perform a fit and extrapolate the quenched value of  $\chi_T$ . For that reason, we incremented the number of measurements to  $10^4$ , separated by 100 sweeps, and simulated a  $10 \times 64$  lattice for  $\beta = 4$ . This improved the results. In figure 5.2 we show the topological susceptibility as a function of the degenerate fermion mass and in figure 5.3 we show the distribution of the configurations. From an extrapolation we obtain

$$\chi_T^{\text{que}} = 0.0274(2)g^2. \quad (5.22)$$

Now, we substitute eq. (5.15) in eq. (5.5) and solve for  $F_\pi$

$$F_\pi^2 = \chi_T^{\text{que}} \frac{2\pi}{g^2}. \quad (5.23)$$

Using the result in eq. (5.22) yields

$$F_\pi = 0.4149(15). \quad (5.24)$$

$\chi_T$  has been obtained in the Schwinger model before. In table 5.1 table we show some values available in the literature together with  $F_\pi$  computed by means of eq. (5.23). We observe that the topological susceptibility value in the literature is in the range 0.023-0.030, so our result is consistent.

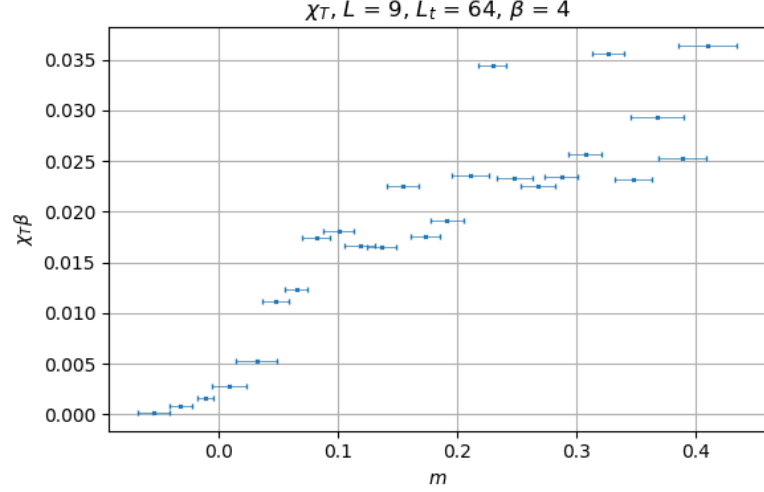
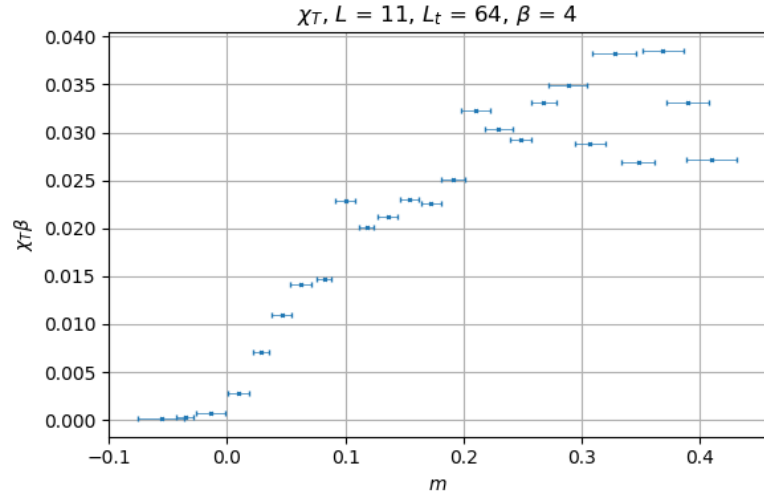
(a)  $\chi_T$  for  $L = 9$  and  $L_t = 64$ (b)  $\chi_T$  for  $L = 11$  and  $L_t = 64$ 

Figure 5.1: Topological susceptibility as a function of the fermion mass  $m$ , computed for  $10^3$  measurements with 10 sweeps between each of them.  $\chi_T$  does not have a clear behavior for this amount of measurements.

We compare our result with the one obtained in the  $\delta$ -regime:  $F_\pi = 0.6688(5)$ . Both of them differ by a factor of 1.6. This shows an inconsistency between the two methods used to measure  $F_\pi$ . However, the method presented in the last chapter was applied to different lattice sizes and values of  $\beta$ , which gives more credibility. On the other hand, the computation of  $F_\pi$  through the topological susceptibility and the WV formula, was only done with one lattice of size  $10 \times 64$  and  $\beta = 4$ , but with high statistics. The amount of measurements used to compute  $\chi_T$  increases the time of each simulation to several days, making it difficult to obtain several results. Moreover, let us remember that the actual decay constant involved in the WV formula is the  $\eta'$ , which is approximated by  $F_\pi$  for large  $N_c$ . This could also explain the discrepancy. Still, further investigation, regarding this issue and simulations with different lattice sizes and high statistics, is needed in order to revise whether the value of  $F_\pi$  obtained with the Witten-Veneziano formula is compatible with the result in the  $\delta$ -regime.

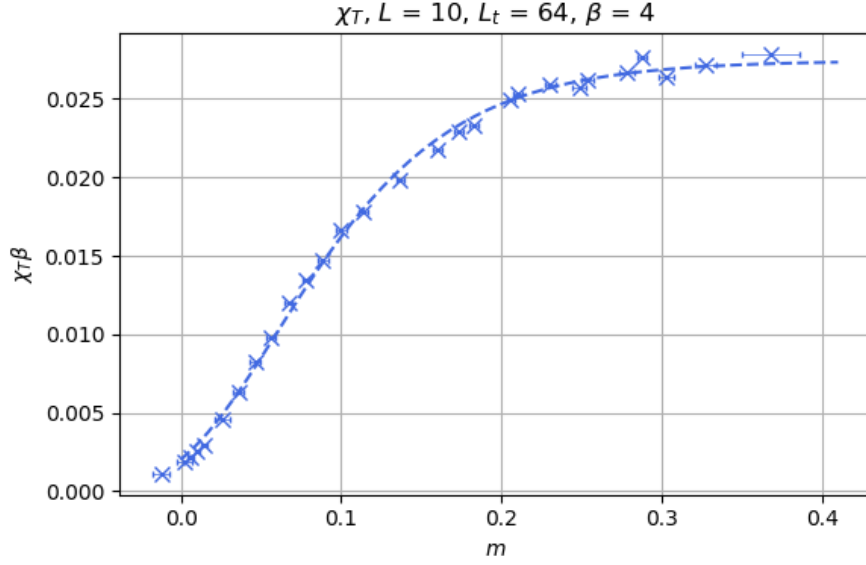
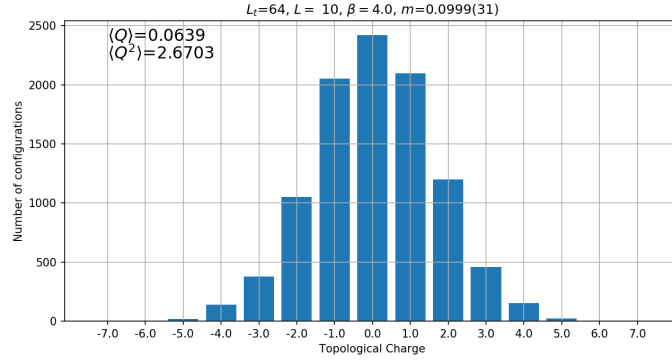
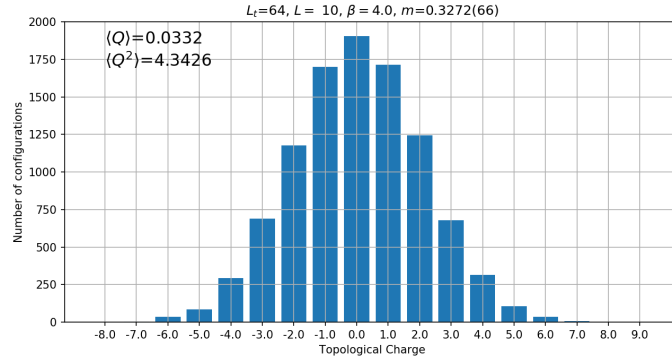


Figure 5.2: Topological susceptibility as a function of the degenerate fermion mass obtained with  $10^4$  measurements. A function of the form  $y = ae^{-be^{-cx}}$  was fitted to the data in order to extract the value of  $\chi_T$  when  $m \rightarrow \infty$ . The only relevant parameter of the fit is  $a = 0.0274(2)$ , since it is equal to  $\chi_T^{\text{que}}/g^2 = \chi_T^{\text{que}}\beta$ . The results are in lattice units.



(a) Configurations sorted by their topological charge for  $m = 0.0999(31)$



(b) Configurations sorted by their topological charge for  $m = 0.3272(66)$

Figure 5.3: Distribution of the Monte Carlo configurations in different topological sectors for  $\beta = 4$ . We see approximately a Gaussian distribution.  $m$  denotes the degenerate PCAC fermion mass. When the mass is smaller, we have less topological sectors

## *Bibliography*

---

- [1] E. Witten. Current Algebra Theorems for the U(1) Goldstone Boson. *Nucl. Phys. B*, 156:269–283, 1979.
- [2] G. Veneziano. U(1) Without Instantons. *Nucl. Phys. B*, 159:213–224, 1979.
- [3] P.A. Zyla et al. Review of Particle Physics. *Prog. Theor. Exp. Phys.*, 2020(8):083C01, 2020.
- [4] E. Seiler. Some more remarks on the Witten-Veneziano formula for the eta-prime mass. *Phys. Lett. B*, 525:355–359, 2002.
- [5] S. Dür, Z. Fodor, C. Hoelbling, and T. Kurth. Precision study of the SU(3) topological susceptibility in the continuum. *JHEP*, 04:055, 2007.
- [6] C. R. Gattringer, I. Hip, and C. B. Lang. Quantum fluctuations versus topology: A Study in U(1)-2 lattice gauge theory. *Phys. Lett. B*, 409:371–376, 1997.
- [7] I. Bautista, W. Bietenholz, A. Dromard, U. Gerber, L. Gonglach, C. P. Hofmann, H. Mejía, and M. Wagner. Measuring the Topological Susceptibility in a Fixed Sector. *Phys. Rev. D*, 92(11):114510, 2015.
- [8] S. Dür and C. Hoelbling. Scaling tests with dynamical overlap and rooted staggered fermions. *Phys. Rev. D*, 71:054501, 2005.